

Wireless health monitoring of stay cable using piezoelectric strain response and smart skin technique

Jeong-Tae Kim*, Khac-Duy Nguyen and Thanh-Canh Huynh

Department of Ocean Engineering, Pukyong National University, Busan, Korea

(Received January 29, 2013, Revised June 15, 2013, Accepted June 20, 2013)

Abstract. In this paper, wireless health monitoring of stay cables using piezoelectric strain sensors and a smart skin technique is presented. For the cables, tension forces are estimated to examine their health status from vibration features with consideration of temperature effects. The following approaches are implemented to achieve the objective. Firstly, the tension force estimation utilizing the piezoelectric sensor-embedded smart skin is presented. A temperature correlation model to recalculate the tension force at a temperature of interest is designed by correlating the change in cable's dynamic features and temperature variation. Secondly, the wireless health monitoring system for stay cables is described. A piezoelectric strain sensor node and a tension force monitoring software which is embedded in the sensor are designed. Finally, the feasibility of the proposed monitoring technique is evaluated on stay cables of the Hwamyung Grand Bridge in Busan, Korea.

Keywords: stay cable; tension force; structural health monitoring; wireless; piezoelectric strain; Imote2

1. Introduction

Cables are the critical structural components of cable supported structures such as cable-stayed bridges, suspension bridges. For those bridges, cable systems carry most of the loads of decks and transfer those loads to foundations through pylons. Stay cables are flexible components, and they are subjected to various repeated load conditions such as vehicle traffic, wind and temperature variation. As a result, stress relaxation in cables due to loosening of cable anchorages can strongly occur and that may lead to significant reduction of loading capacity of the structures. Therefore, health monitoring of stay cables is very essential to ensure the structural integrity and operational safety of the cable-stayed structures.

For health monitoring of stay cables, vibration-based techniques are widely used since these approaches are simple and reliable. Utilizing dynamic characteristics of vibrated cables, many methods of cable vibration assessment and cable force estimation have been proposed and successfully evaluated not only on small scale cables but also on full scale cables (Zui *et al.* 1996, Kim and Park 2007). Up to date, most of the researchers have utilized acceleration features to estimate cable forces. Only a few studies have considered strain responses for monitoring cable forces. Li *et al.* (2009) utilized optical fiber Bragg grating (FBG) strain sensors to monitor cable

*Corresponding author, Professor, E-mail: idis@pknu.ac.kr

tension force based on a direct method. Ma and Wang (2009) used dynamic strain of cables measured by FBG strain sensors or strain gauges for cable force monitoring. However, the data acquisition systems associated with those kinds of sensors are expensive, complicated and heavy, that limits their applicability to real structural cables.

Recently, the interest in developing wireless smart sensor nodes for efficient SHM systems has been increasing. The advantages of wireless sensor systems over conventional sensor systems have been discussed by many researchers (Spencer *et al.* 2004, Lynch and Loh 2006, Nagayama *et al.* 2007, Kim *et al.* 2011). For stay cables, the cost associated with wiring the conventional system can be greatly reduced by the adoption of wireless sensor nodes. Furthermore, the autonomous operation of the wireless system which is enabled by on-board computation units allows the long-term health monitoring for stay cables without experts' offline interference (Cho *et al.* 2010).

Over the last two decades, piezoelectric materials have been widely adopted for SHM applications (Park *et al.* 2003). The piezoelectric materials are commonly used for active monitoring of critical structural members (Liang *et al.* 1996, Park *et al.* 2001, Bhalla and Soh 2003, Kim *et al.* 2006, Nguyen and Kim 2012). Although the materials are capable for strain sensing, they can not represent static structural responses since they generate only dynamic signals. However, those materials can be useful for vibration-based cable force monitoring since only dynamic parameters of the cable are needed. One of the advantages of the piezoelectric strain-based approach over the acceleration-based one is that it is simple to utilize piezoelectric strain sensors for measuring the voltage induced from structural deformation. The piezoelectric strain sensors do not need either power supply or exciting input signal, which will be beneficial for the wireless SHM application. Moreover, the piezoelectric strain sensors and the associated signal acquisition devices are very cheap compared to acceleration-based or electrical strain-based systems.

Many researchers have examined that temperature variation is the key factor affecting the accuracy of damage detection results (Ni *et al.* 2005, Kim *et al.* 2003, Kim *et al.* 2007, Hong *et al.* 2012). They have attempted to correlate modal properties with temperature change, and also to develop system identification models that could separate the influence of temperature change from damage-induced changes in modal parameters. For stay cables under temperature variation, some efforts have been made to discriminate temperature-induced changes in cables' vibration responses from damage-induced ones (Treyssede 2009, Chen *et al.* 2012).

This paper presents the wireless health monitoring of stay cables using piezoelectric strain sensors and a smart skin technique. For the cables, tension forces are estimated to examine their health status from vibration features with consideration of temperature effects. Firstly, the tension force estimation utilizing the piezoelectric sensor-embedded smart skin is presented. A temperature correlation model to adjust the tension force for a specified temperature is designed by correlating the change in cable's dynamic features and temperature variation. Secondly, the wireless health monitoring system for stay cables is described. A piezoelectric strain sensor node and a tension force monitoring software which is embedded in the sensor are designed. Finally, the feasibility of the proposed monitoring technique is evaluated on stay cables of the Hwamyung Grand Bridge in Busan, Korea.

2. Piezoelectric strain-based tension force estimation

2.1 Piezoelectric strain response

The principle of piezoelectric materials (PZT) as strain sensors is shown in Fig. 1. As direct effect of the materials, an electrical displacement (related directly to electrical current) is induced since a mechanical stress (or strain) is applied to a piezoelectric sensor. The strain-charge relation for a piezoelectric material can be expressed as follows (Sirohi and Chopra 2000)

$$D_3 = e_{33}^\sigma E_3 + d_{31} \sigma_1 \quad (1a)$$

$$\varepsilon_1 = \frac{\sigma_1}{Y^E} + d_{31} E_3 \quad (1b)$$

where D_3 is the electric displacement; e_{33}^σ is the dielectric constant of the piezoelectric patch; E_3 is the applied external electric field in direction-3 at zero stress; d_{31} is the piezoelectric coupling constant; σ_1 is the stress in direction-1, ε_1 is the strain in direction-1, Y^E is the Young's modulus of the material at zero-electric field. If the PZT patch is surface-bonded on a host structure, the strain of the PZT patch can be expressed in terms of voltage measured from its terminals as

$$\varepsilon_1 = \left(\frac{e_{33}^\sigma}{d_{31} t_p Y^E} \right) V = k_p V \quad (2)$$

where V is the output voltage across the terminals of the PZT patch; t_p is thickness of the PZT patch; k_p is the scale factor between strain and voltage which depends on the characteristics of the PZT patch. The scale factor for a PZT patch can be obtained experimentally by correlating voltage signal of the PZT sensor with strain signal of a commercial strain sensor (Nguyen *et al.* 2013).

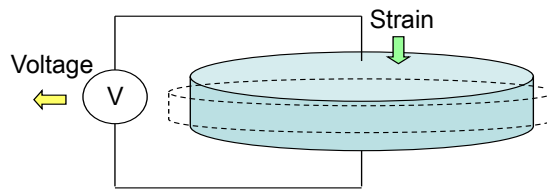


Fig. 1 Direct piezoelectric effect

2.2 PZT-embedded smart skin for cable strain measurement

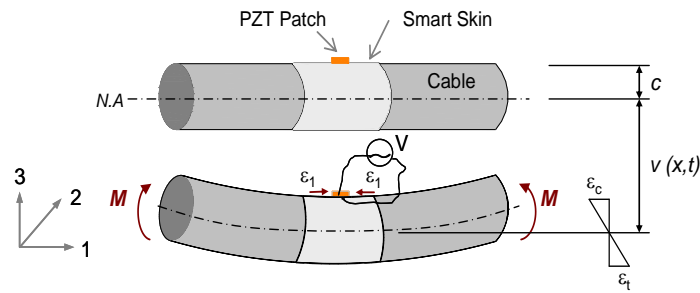
In real cable-stayed bridges, it is not allowed to bond PZT sensors directly on stay cables. Also, bonding condition between the PZT sensors and cable surfaces which are made of polyethylene (PE) is not well maintained. In order to overcome those difficulties, a PZT-embedded smart skin is designed as shown in Fig. 2. A PZT sensor is bonded on a skin plate which tightly covers the cable. As shown in Fig. 2(b), the deformation of the smart skin is secured by the static friction in the interface between the skin and the cable. For design specification, the skin plate should be flexible

and should have low mass in order not to affect response of the cable. Also, its thickness should be small enough compared with the cable section and its surface should have large frictional coefficient in order to guarantee the accuracy of strain measurement.

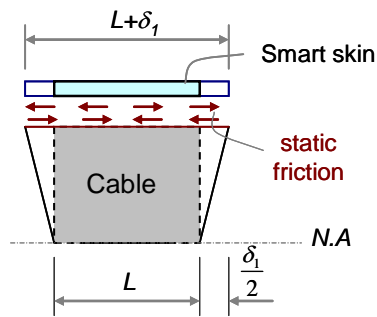
In order to utilize Eq. (2), it is assumed that only 1-D strain is contributed to the charge generation and that there is no loss of strain in the bond layer. Those assumptions are highly satisfied for stay cables since their vibration causes longitudinal strain induced by bending (flexural strain) with large amplitudes. When the cable is vibrated in-plane, dynamic flexural strain of the cable can be expressed as

$$\varepsilon_1 = \frac{Mc}{EI} = \frac{\partial^2 v(x,t)}{\partial x^2} c \quad (3)$$

where M is the bending moment of the cable caused by the cable vibration, EI is the flexural stiffness of the cable, $v(x,t)$ is the displacement of the cable in the direction perpendicular to length of the cable, and c is the distance of the PZT patch from the neutral axis of the cable. As shown in Fig. 2, when the cable is deformed, a voltage is generated due to the PZT's strain. It is worth to note that, the PZT sensor also measure longitudinal modes of the cable. However, the longitudinal modes have very high frequencies compared with the in-plane flexural modes.



(a) Piezoelectric strain vs cable vibration



(b) Force equilibrium condition

Fig. 2 Schematic of PZT-cable interaction via smart skin

2.3 Health assessment of stay cable

2.3.1 Frequency-based cable force model

Over the last two decades, several methods have been proposed for the estimation of cable force by measuring natural frequencies of cables (Shimada 1995, Zui *et al.* 1996). Among those, the method proposed by Zui *et al.* (1996) considers effects of both flexural rigidity and cable-sag on cable force estimation. The tension force of a stay cable can be estimated using the practical formulas as follows

Case 1. Cable with small sag ($\Gamma \geq 3$)

$$F = 4m(f_1 L)^2 \left[1 - 2.2 \frac{C}{f_1} - 0.55 \left(\frac{C}{f_1} \right)^2 \right]; \zeta \geq 17 \quad (4a)$$

$$F = 4m(f_1 L)^2 \left[0.865 - 11.6 \left(\frac{C}{f_1} \right)^2 \right]; 6 \leq \zeta \leq 17 \quad (4b)$$

$$F = 4m(f_1 L)^2 \left[0.828 - 10.5 \left(\frac{C}{f_1} \right)^2 \right]; \zeta \leq 6 \quad (4c)$$

Case 2. Cable with large sag ($\Gamma \leq 3$)

$$F = m(f_2 L)^2 \left[1 - 4.4 \frac{C}{f_2} - 1.1 \left(\frac{C}{f_2} \right)^2 \right]; \zeta \geq 60 \quad (5a)$$

$$F = m(f_2 L)^2 \left[1.03 - 6.33 \frac{C}{f_2} - 1.58 \left(\frac{C}{f_2} \right)^2 \right]; 17 \leq \zeta \leq 60 \quad (5b)$$

$$F = m(f_2 L)^2 \left[0.882 - 85 \left(\frac{C}{f_2} \right)^2 \right]; \zeta \leq 17 \quad (5c)$$

Case 3. Very long cable

$$F_n = \frac{4m}{n^2} (f_n L)^2 \left[1 - 2.2_n \frac{C}{f_n} \right]; \zeta > 200 \quad (6)$$

where f_1, f_2, f_n are respectively measured natural frequencies corresponding to first, second and n^{th} mode ($n \geq 2$); $C = \sqrt{EI/(mL^4)}$; $\zeta = \sqrt{F/(EI)L}$;

$\Gamma = \sqrt{(mgL)/(128EA\delta^3 \cos^5 \theta)} [(0.31\zeta + 0.5)/(0.31\zeta - 0.5)]$; EI is the flexural rigidity of cable; L is the span length of cable; m is the mass of cable per unit length; δ is sag-to-span ratio which can

be calculated as: $\delta = mgL/(8F)$; and θ is inclination angle of cable. If cable tension is estimated using Eq. (6) for NM modes, the average value of cable tension is calculated as

$$F = \frac{1}{NM} \sum_{n=2}^{NM} F_n \quad (7)$$

2.3.2 Temperature-correlation for cable force model

For a stay cable subjected to two different temperatures, the axial extension of the cable due to temperature variation (e.g., $\Delta L_T = \alpha_T L \Delta T$) is equivalent to the deformation by the change in tension force at anchorage (e.g., $\Delta F = -EA \Delta L_T / L = -\alpha_T EA \Delta T$); where α_T is the coefficient of linear thermal expansion of the cable, ΔT is the temperature variation, and d is the axial rigidity of the cable. The change in tension force can be simplified in a reduced order as

$$\Delta F \approx g(m, L) \Delta f_k^2 / k^2 \quad (8)$$

where $\Delta f_k^2 = f_k^{*2} - f_k^2$ is the change in square of natural frequency; f_k and f_k^* is the k^{th} natural frequencies of the cable before and after tension force change, respectively; k is the mode number; and $g(m, L)$ represents geometric and material quantities of the cable. Hence, the change in square of natural frequency due to temperature variation is expressed as follows

$$\Delta f_k^2 \approx -\beta_k \Delta T \quad (9)$$

where β_k is temperature correlation index which may be calculated as: $\beta_k = \alpha_T EA k^2 / g(m, L)$. However, since it is difficult to obtain the geometric and material quantities $g(m, L)$ for a real cable, the value of β_k can be estimated from field experiment by correlating the change in natural frequency and temperature variation.

3. Wireless health monitoring system for stay cable

3.1 Piezoelectric strain sensor node

As shown in Fig. 3, a piezoelectric strain sensor node is designed for measuring piezoelectric strain response (i.e., strain-induced voltage). Its core component is the digital filter QF4A512 ADC for signal conditioning with customizable sampling rates. It is interfaced with the Imote2 sensor platform via SPI protocol that transmits the measured signal to the main CPU. Other components of a complete wireless sensor node are integrated in the Imote2 platform such as onboard computation, data storage, wireless communication and power supply management units. The Imote2 has a low power, high speed PXA27x processor and a wireless radio. It also has 256 kB SRAM, 32 MB SDRAM, and 32 MB FLASH. As shown in Fig. 4, the SHM-A sensor board developed by Rice *et al.* (2010) was modified to acquire piezoelectric strain signal by hooking up the PZT sensor to its external channel. The modified sensor board SHM-A(S) is capable of measuring both 3-D acceleration and PZT dynamic strain. Temperature and humidity also can be measured by embedded sensor SHT11 on the SHM-A(S).

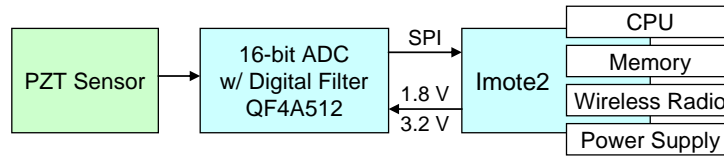


Fig. 3 Design schematic of wireless piezoelectric strain acquisition sensor node

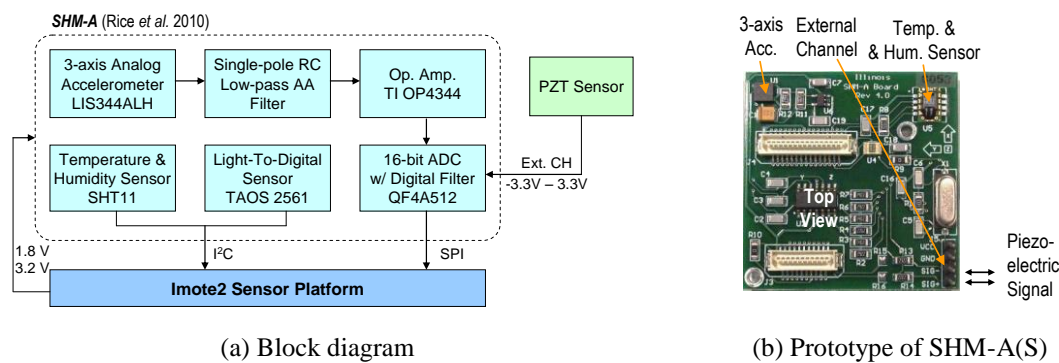


Fig. 4 SHM-A(S) for the use of MEM accelerometer and piezoelectric strain sensor

3.2 Tension force monitoring software

The embedded software for monitoring tension force is programmed for the sensor node according to the UIUC ISHMP Services Toolsuite (Illinois Structural Health Monitoring Project 2010) and PKNU SSeL-SHM Tools (Kim *et al.* 2011). As schematized in Fig. 5, the *RemoteSensing* component of the ISHMP Services Toolsuite is implemented for cable strain sensing. Also, temperature is monitored by the embedded *ReadTemp* component. For long-term operation, the sensor nodes are embedded with the *ChargerControl* component to harvest environmental energies such as wind energy or solar energy. The *AutoMonitor* component is embedded to the gateway node to periodically wake up the sensor system and let the sensor nodes measure structural responses. More detailed information on the *ChargerControl* and *AutoMonitor* components can be found in Miller *et al.* (2010) and Rice and Spencer (2009), respectively.

Once vibration signal and temperature are recorded, cable tension is estimated by the *CableMonitor* component of the SSeL-SHM Tools. Similar to the one presented by Sim *et al.* (2011), the operation process of the *CableMonitor* is schematized in Fig. 6. The procedure performs three major tasks including power spectral density (PSD) calculation, natural frequency calculation, and tension force estimation as follows:

3.2.1 Power spectral density calculation

The recorded signal is transformed into the PSD according to Bartlett's procedure as follows (Bendat and Piersol 1993)

$$S_{xx}(f) = \frac{1}{n_d T} \sum_{i=1}^{n_d} |X_i(f, T)|^2 \quad (10)$$

where X_i is the dynamic response transformed into the frequency domain (FFT transform); n_d is the number of divided segments in the time history response; and T is the data length of a divided segment. Here, a Hanning window with the number of FFT of 2048 is used to calculate X_i from the time history response. Then, the change in the PSD due to structural change is quantified by the correlation coefficient (CC) of PSD as

$$\rho_{xy} = \frac{E[S_{xx}(f)S_{yy}(f)] - E[S_{xx}(f)]E[S_{yy}(f)]}{\sigma_{S_{xx}}\sigma_{S_{yy}}} \quad (11)$$

where $E[\bullet]$ is the expectation operator; $S_{xx}(f)$ and $S_{yy}(f)$ are the PSDs of two time history signals before and after structural change, respectively; and $\sigma_{S_{xx}}$, $\sigma_{S_{yy}}$ are the corresponding standard deviations of the PSDs, respectively.

3.2.2 Natural frequency calculation

Natural frequencies are obtained from the automated peak-picking algorithm. The basic concept of the algorithm is to search the local maxima of the PSD curve, which represent natural frequencies. Assuming that natural frequencies of the cable are periodic and the allowable loss of tension force is as maximal as 80% of the design force, the automated peak-picking is performed as follows: Firstly, the size of frequency band (df) is selected as

$$df \leq (f_1)_{20} = \sqrt{F_{20}/(4mL^2)} \quad (12)$$

where $(f_1)_{20}$ is the fundamental frequency corresponding to 20% of the design force (F_{20}). Secondly, the entire frequency range (i.e., from 0 to the cut-off frequency, f_c) is divided into N number of sub-frequency ranges, in which $N = f_c / df$. For example, sub-frequency range 1 is $0 \sim df$, sub-frequency range 2 is $df \sim 2df$, ..., and sub-frequency range N is $(f_c - df) \sim f_c$. Finally, by examining each sub-frequency range, the natural frequency is picked if its magnitude is the largest in the range and at least 5 times greater than the magnitude mean. Sometimes, the false natural frequency can be picked together with the true one if the peak is very close to the boundary of a sub-frequency range. To avoid this situation, if the gap between two subsequent picked frequencies is less than $0.5df$, only the greater peak is selected as the natural frequency.

3.2.3 Tension force estimation

Once the natural frequencies are obtained as described previously, they are adjusted to the equivalent values at a specified temperature using Eq. (9). Then, the tension force is estimated in the following three steps. At first, the raw value of cable force (F_s) is calculated using the fundamental natural frequency (f_1) based on the string theory as: $F_s = 4m(f_1 L)^2$. Next, values of cable parameters (δ , ξ , Γ) are determined using the tension force calculated in step 1. Then, the final tension force is estimated using Eqs. (4)-(7) depending on the values of δ , ξ , Γ

calculated in step 2. Once the computation process is finished, the estimated tension force is transmitted to the gateway node at base station.

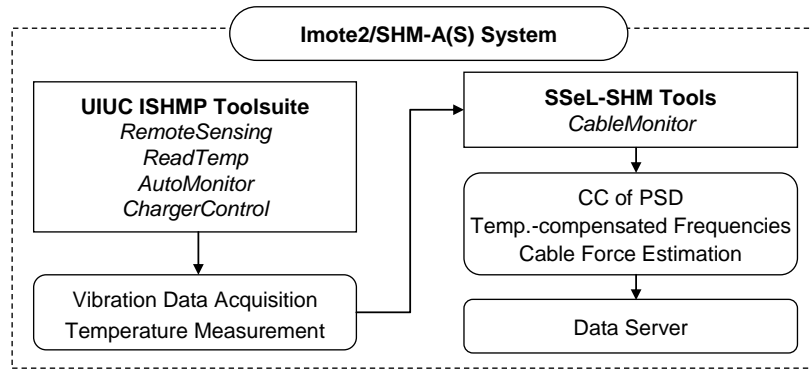


Fig. 5 Schematic of wireless monitoring software for stay cables

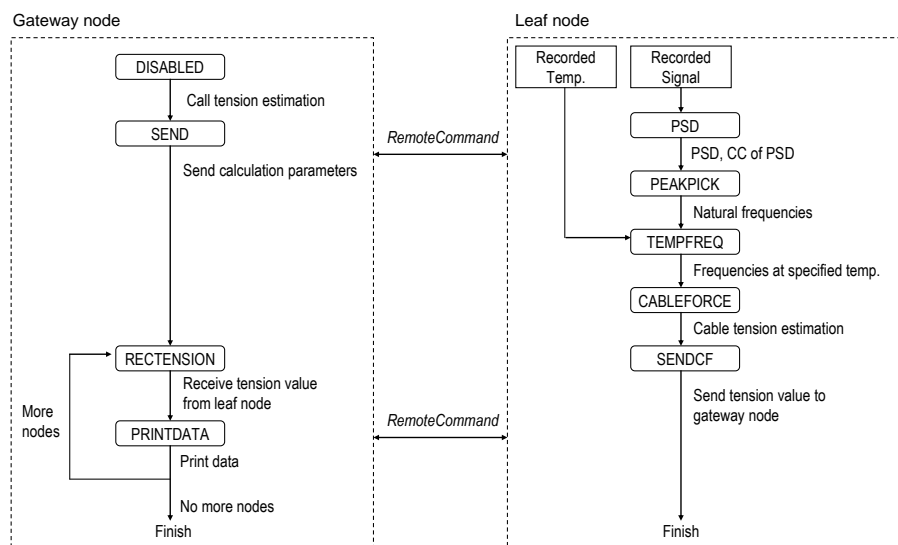


Fig. 6 Flowchart of CableMonitor Component

4. Experimental evaluation on real stay cables

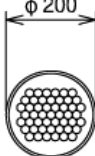
4.1 Experiment description

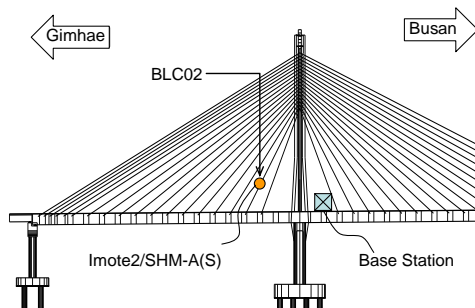
The feasibility of the proposed cable tension monitoring system was evaluated on stay- cables of the Hwamyung Grand Bridge, which is the longest cable-stayed bridge with prestressed concrete box girder in Korea, as shown in Fig. 7. This bridge has also been selected for the implementation of a multi-scale wireless SHM system using Imote2-platformed sensor technology

(Ho *et al.* 2012). The bridge consists of three spans (a 270-m mid span and two 115-m side spans) which are supported by 72 multi-strand type stay cables. Among the 72 cables, a short cable BLC02 at the span toward Gimhae side was selected for the evaluation test. The selected cable is comprised of 49 stainless steel 1x7 strands, and its length is 44.89 m. The cable is covered by a high-density polyethylene (HDPE) duct with the diameter of 200 mm. More detailed specifications of the cable are given in Table 1.

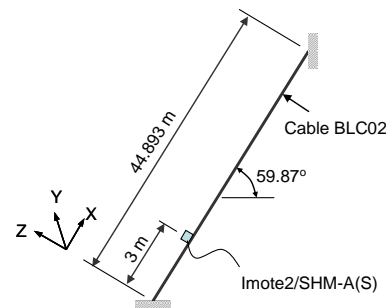
At location of 3 m from the cable end, a PZT sensor (FT-35T-2.8A1) was installed to the cable by bonding onto a smart skin, as shown in Figs. 7 and 8. The PZT sensor was connected to an Imote2/SHM-A(S) for strain monitoring. Here the smart skin was designed as an aluminum tube with 0.4 mm thickness. The aluminum tube was thin, flexible, and almost weightless compared to cable's mass. The quality of contact interface between the tube and the cable is maintained by bolt connection on the tube. For validation, in-plane acceleration response (i.e., z-directional response) was also measured by the MEMS accelerometer integrated in the SHM-A(S). The base station including a gateway node and a PC was installed at the nearest pylon as shown in Fig. 7(a). The sensor node and the gateway node were placed in plastic boxes which have waterproof rubber gaskets for preventing the nodes from sun-heating, absorbent and other environmental effects such as rain, wind and dust. The sensor node was powered by a Li-ion polymer rechargeable battery (Powerizer 3.7 V, 10000 mAh). A solar panel (SPE-350-6) was mounted on the sensor box to harvest the solar energy and recharge the battery. The sensor node was automatically activated every two hours, and measured acceleration and dynamic strain in 10 minutes with a sampling rate of 25 Hz and a cut-off frequency of 10 Hz. The temperature was also measured by the sensor node every two hours.

Table 1 Specification of cable BLC02 of the Hwamyung Grand Bridge

Cable cross section		Length (m)	44.893
Strand Num	49	Tensile strength (kN)	13671
Nominal area (mm ²)	7350	Elastic modulus (GPa)	195
Moment of inertial (mm ⁴)	4.3×10^6	Unit mass (kg/m)	67.54



(a) Hwamyung Grand Bridge



(a) Hwamyung Grand Bridge

Fig. 7 Sensor layout on the Hwamyung Grand Bridge

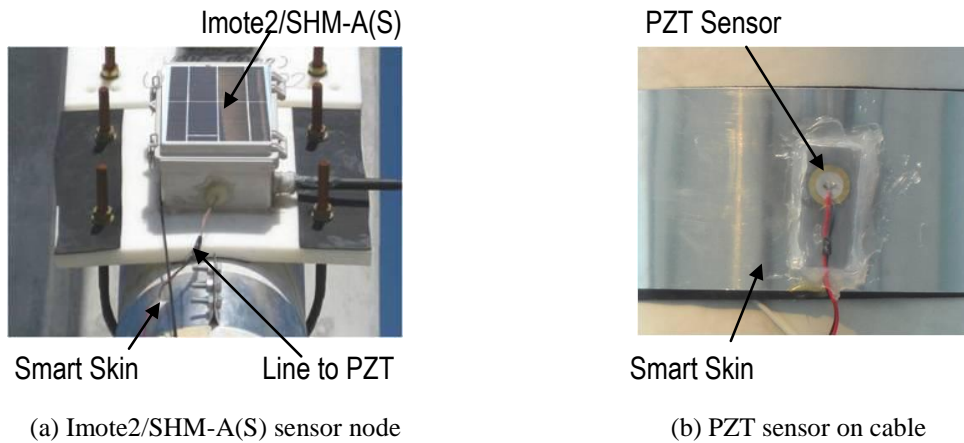


Fig. 8 Experimental setup for cable BLC02

4.2 Performance of automated tension force estimation

Figure 9 shows the dynamic strain and acceleration responses of the cable. The corresponding PSDs of the signals are shown in Fig. 10. Sharp peaks indicating resonant responses of the cable can be clearly seen from the PSDs of both strain and acceleration signals. Natural frequencies of the cable were extracted by the automated peak-picking process as described previously. The fundamental natural frequency corresponding to 20% of the design force ($F_{20} = 966$ kN) is approximated as 1.33 Hz. For picking natural frequencies, eight (8) sub-frequency ranges with 1.25 Hz uniform intervals were made from the original one. Natural frequencies measured by the PZT sensor and the MEMs accelerometer systems are listed in Table 2. It is observed that the natural frequencies measured by the PZT sensor are almost same as those measured by the accelerometer.

Using the natural frequencies of the first mode, cable forces were estimated by the cable force estimation model as described in Eqs. (4)-(7). The cable forces estimated by the accelerometer and the PZT sensor systems are listed in Table 2. It is found that the estimated cable forces using the two sensor types show good agreement each other. In Table 2, also the estimated tension force is compared with the corresponding one obtained from the lift-off test which was carried out during the construction. The difference in tension force between those two tests is about 4.8%.

Table 2 Cable force estimation: acceleration-based vs dynamic strain-based

Signal	Design Force (kN)	Lift-off Force (kN)	Frequency			String Theory F_s (kN)	ξ	Γ	Estimated Force (kN)	Formula
			1 st	2 nd	3 rd					
Strain	4828	4626	2.905	5.701	8.654	4595	105.1	284	4402 (4.8%)	4a
Acc.			2.905	5.688	8.642	4595	105.1	284	4402 (4.8%)	4a

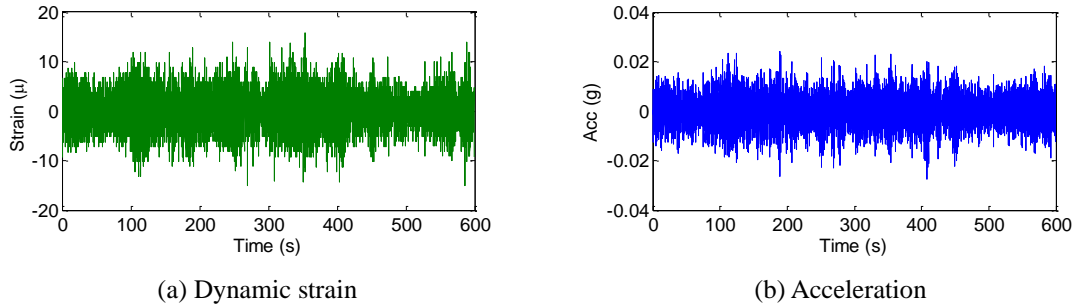


Fig. 9 Time history responses of cable BLC02

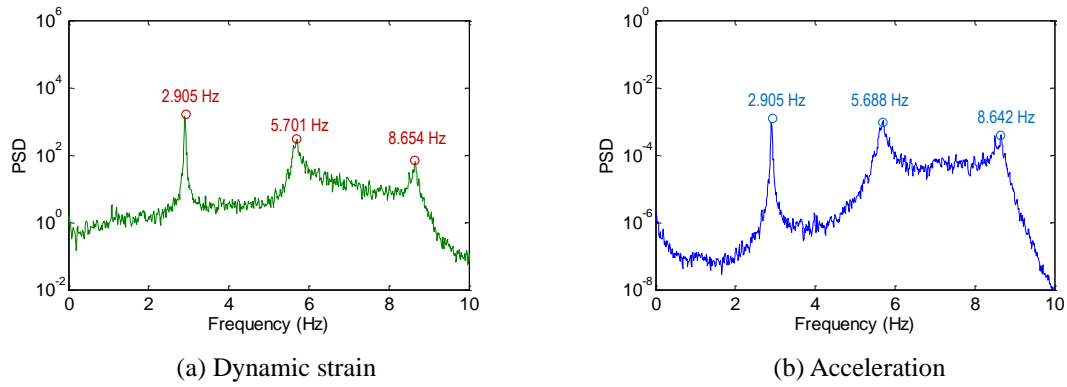
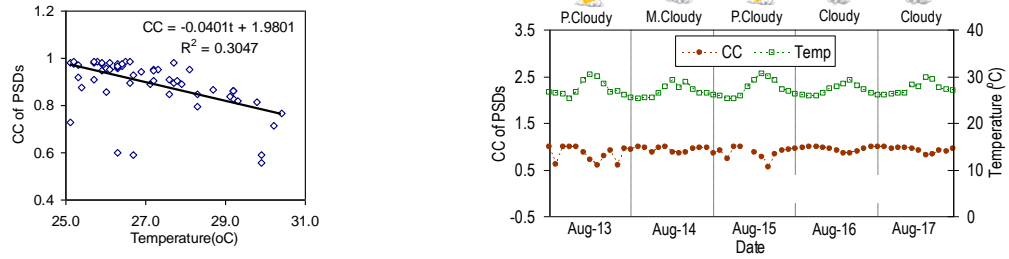


Fig. 10 Frequency responses of cable BLC02

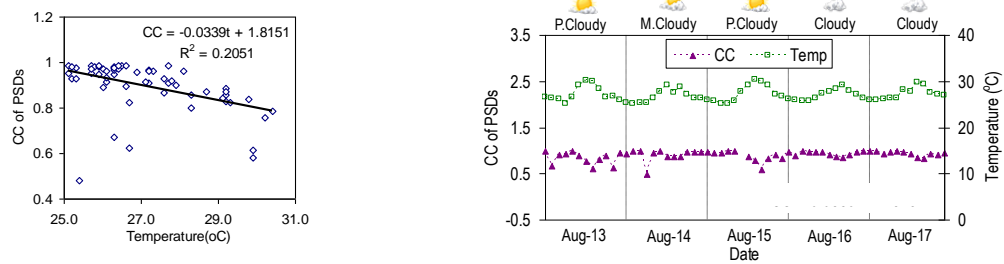
4.3 Temperature effect on cable vibration

The effect of temperature variation on cable vibration was investigated by using the wireless sensor system. Fig. 11 shows the CC of PSDs (calculated by Eq. (11)) versus the temperature change over five-day monitoring period. It is observed that the CC of PSDs consistently changes due to the change in temperature. It is also found the effect of temperature on the PSD of dynamic strain is similar with that on the PSD of acceleration.

Fig. 12 shows the relative changes in the first natural frequency extracted from acceleration and dynamic strain signals versus temperature change in five days. The natural frequency decreases as the temperature goes up, and vice versa. This implies axial stress of the cable is partially released when temperature increases and vice versa. The similarity in the monitoring results with uses of the two signal types proves that the PZT dynamic strain can be used as a vibration feature for cable health monitoring. In order to quantify the effect of temperature variation on vibration responses of cable BLC02, linear relationships between the temperature and the square of the first natural frequency were made according to Eq. (9) with temperature correlation indices as: $\beta_{l,a} = 0.0135$ for the acceleration response and $\beta_{l,s} = 0.0133$ for the PZT strain response.

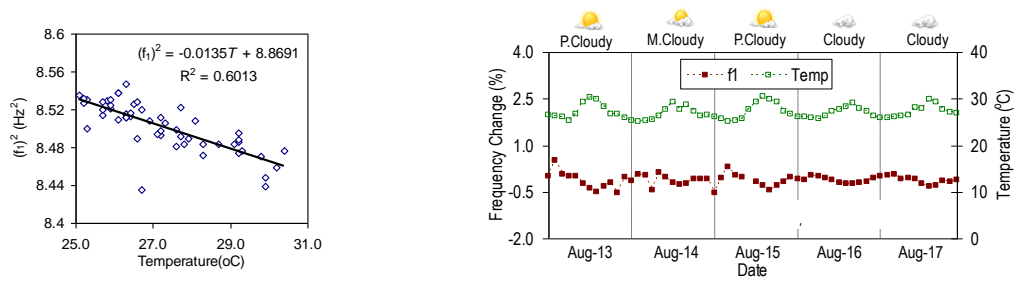


(a) Acceleration

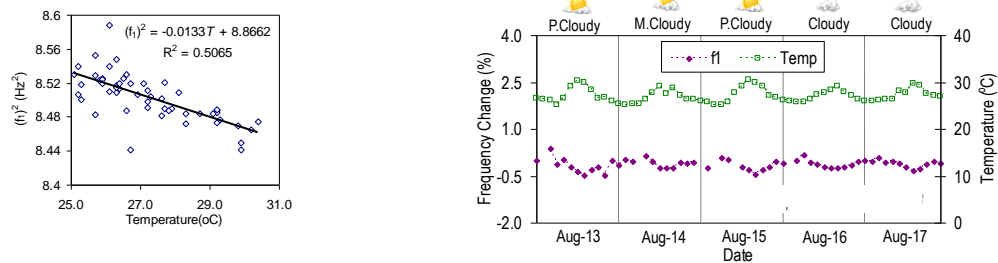


(b) PZT Dynamic Strain

Fig. 11 Changes in CCs of PSDs due to temperature variation on cable BLC02



(a) Acceleration



(b) PZT Dynamic Strain

Fig. 12 Changes in 1st natural frequency due to temperature variation on cable BLC02

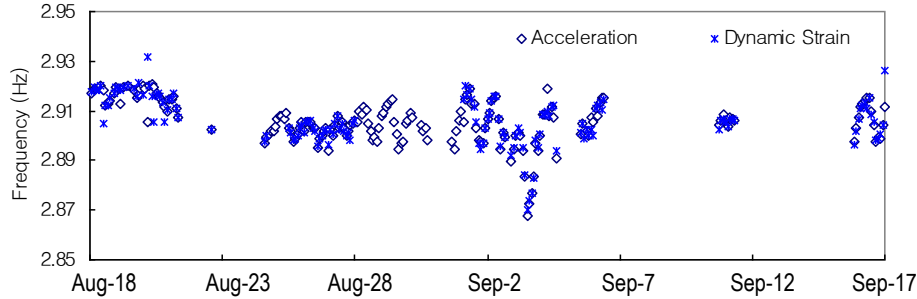


Fig. 13 1st natural frequency of cable BLC02 extracted from acceleration and dynamic strain in one month

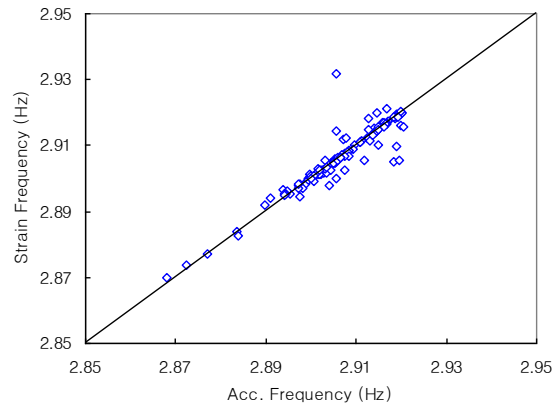


Fig. 14 1st natural frequency: Dynamic Strain vs Acceleration

4.4 Long-term assessment of cable tension force

It is observed that the values of natural frequencies extracted from two signal types are well matched each other.

Long-term tension force monitoring of the selected cable was also carried out by using the wireless sensor system. Fig. 13 shows the first natural frequencies measured in one month. As shown in the figure, data in several periods were missed due to the interruption of power supply for the base station or simply due to data loss. The total amount of measured data is about 200 for acceleration and 160 for dynamic strain. The comparison between the first natural frequencies extracted from dynamic strain signals and those from acceleration signals is illustrated in Fig. 14.

The distribution densities of estimated tension forces of cable BLC02 at the temperatures as they were measured are shown in Fig. 15. It can be seen that the distribution of the tension force obtained from using dynamic strain is matched very well with that from using acceleration. However, the mean value of estimated force is found to be 4405 kN (by using either acceleration or dynamic strain signals) which has about 4.8% difference from the value of the lift-off test. Note that the tension forces from the vibration test were estimated at the temperatures varied from

21.9°C to 44.7°C, while the value from the lift-off test was obtained at -2°C.

In order to examine the accuracy of the estimation more feasibly, the values of the first natural frequency were adjusted with the difference between the measured temperatures and -2°C. Figure 16 shows the distribution of the equivalent estimated tension force at temperature of -2°C. As shown in the figure, the estimation becomes better matched with the value obtained from the lift-off test. The mean values of estimated force are found to be 4625 kN by using dynamic strain and 4631 kN by using acceleration. Those values are found little different from the lift-off result by about 0.02% and 0.11% by using the PZT dynamic strain and acceleration signals, respectively.

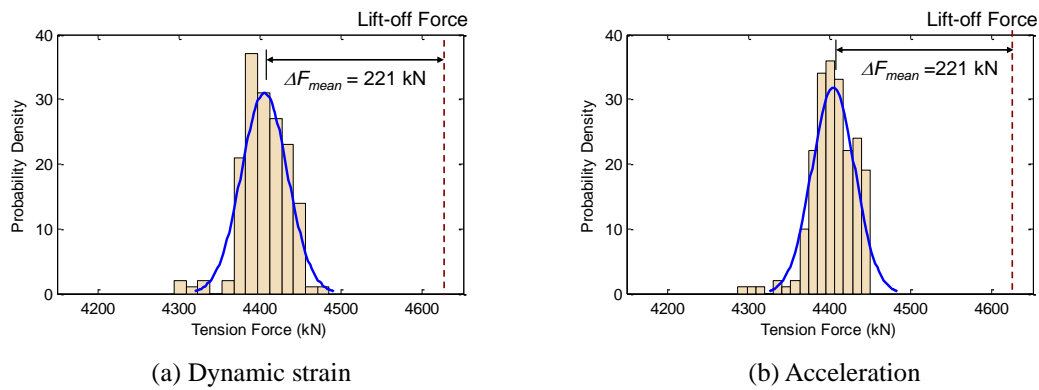


Fig. 15 Distribution of estimated cable force at measured temperatures of 21.9°C to 44.7°C

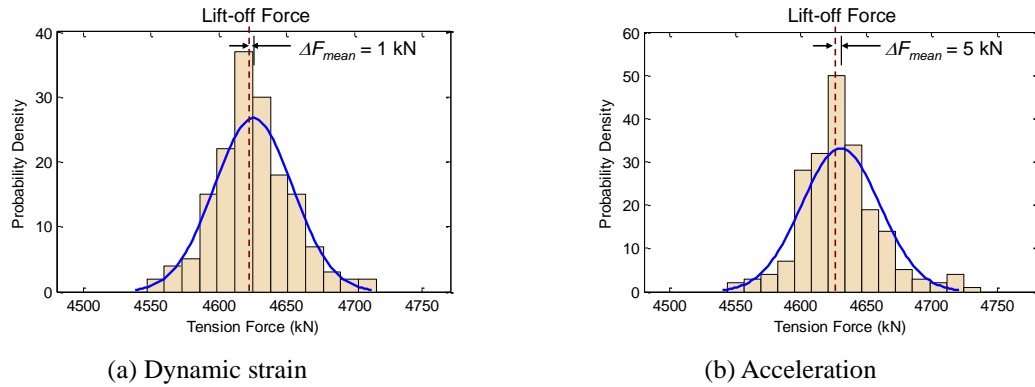


Fig. 16 Distribution of equivalent estimated cable force at -2°C

5. Conclusions

In this study, a wireless monitoring system for assessing health status of stay cables by using piezoelectric strain sensor nodes and PZT-embedded smart skins was developed. The tension force estimation method utilizing the piezoelectric sensor-embedded smart skin was first presented. A temperature correlation model to adjust the tension force estimation for a specified temperature

was designed by correlating the change in cable's dynamic features and temperature variation. Then, the hardware and operating software of a wireless health monitoring system were designed for stay cables. The feasibility of the monitoring system was evaluated on stay cables of the Hwamyung Grand Bridge in Busan, Korea.

From the experiment results, the following conclusions have been made. Vibration responses of the cable were sensitively measured by the PZT sensor embedded on the smart skin. The natural frequencies measured by the wireless piezoelectric strain sensor were agreed well with those measured by the MEMs accelerometer on the Imote2/SHM-A(S). Also, the cable tension forces were successfully estimated and monitored by the proposed strain system. The differences between the equivalent estimated forces with regard to temperature variation and the value obtained from the lift-off test are reasonably small.

The future works are remained to investigate the sensitivity of piezoelectric strain signals to cable vibration. Also, since strain of cables seem to be much influenced by vibration of decks, effect of parametric excitation should be examined and eliminated from the strain signals.

Acknowledgements

This work was supported by the Pukyong National University Research Abroad Fund in 2012 (C-D-2012-0915).

References

- Bhalla, S. and Soh, C.K. (2003), "Structural impedance based damage diagnosis by piezo-transducers", *Earthq. Eng. Struct. D.*, **32**(12), 1897-1916.
- Bendat, J.S. and Piersol, A.G. (1993), *Engineering applications of correlation and spectral analysis*, New York, NY, Wiley-Interscience.
- Chen, C.C., Wu, W.H. and Liu, C.Y. (2012), "Effects of temperature variation on cable forces of an extradosed bridge", *Proceeding of the 6th European Workshop on Structural Health Monitoring*, Germany.
- Cho, S., Lynch, J.P., Lee, J.J. and Yun, C.B. (2010), "Development of an automated wireless tension force estimation system for cable-stayed bridges", *J. Intell. Mat. Syst. Str.*, **21**(1), 361-375.
- Kim, B.H. and Park, T. (2007), "Estimation of cable tension force using the frequency-based system identification method", *J. Sound Vib.*, **304**, 660-676.
- Kim, J.T., Yun, C.B. and Yi, J.H. (2003), "Temperature effects on frequency-based damage detection in plate-girder bridges", *J. Civil Eng. - KSCE*, **7**(6), 725-733.
- Kim, J.T., Na W.B., Park, J.H. and Hong, D.S. (2006), "Hybrid health monitoring of structural joints using modal parameters and EMI signatures", *Proceedings of the SPIE*, San Diego, USA.
- Kim, J.T., Park, J.H. and Lee B.J. (2007), "Vibration-based damage monitoring in model plate-girder bridges under uncertain temperature conditions", *Eng. Struct.*, **29**, 1354-1365.
- Kim, J.T., Park, J.H., Hong, D.S. and Ho, D.D. (2011), "Hybrid acceleration-impedance sensor nodes on Imote2-platform for damage monitoring in steel girder connections", *Smart Struct. Syst.*, **7**(5), 393-416.
- Ho, D.D., Lee, P.Y., Nguyen, K.D., Hong, D.S., Lee, S.Y., Kim, J.T., Shin, S.W., Yun, C.B. and Shinozuka, M. (2012), "Solar-powered multi-scale sensor node on Imote2 platform for hybrid SHM in cable-stayed bridge", *Smart Struct. Syst.*, **9**(2), 145-164.
- Hong, D.S., Nguyen, K.D., Lee, I.C. and Kim, J.T. (2012), "Temperature-compensated damage monitoring by using wireless acceleration-impedance sensor nodes in steel girder connection", *Int. J. Distrib. Sens. N.*,

2012, 1-12.

- Li, H., Ou, J. and Zhou, Z. (2009), "Applications of optical fibre Bragg gratings sensing technology-based smart stay cables", *Opt. Laser. Eng.*, **47**, 1077-1084.
- Liang, C., Sun, F.P. and Rogers, C.A. (1996), "Electro-mechanical impedance modeling of active material systems", *Smart Mater. Struct.*, **5**(2), 171-186.
- Lynch, J.P. and Loh, K.J. (2006), "A summary review of wireless sensors and sensor networks for structural health monitoring", *Shock Vib.*, **38**(2), 91-128.
- Ma, C.C. and Wang, C.W. (2009), "Transient strain measurements of a suspended cable under impact loadings using fiber bragg grating sensors", *IEEE Sens. J.*, **9**(12), 1998-2007.
- Miller, T.I., Spencer, B.F., Li, J. And Jo, H. (2010), *Solar energy harvesting and software enhancements for autonomous wireless smart sensor networks*, NSEL Report Series, NSEL-022.
- Nagayama, T., Sim, S.H., Miyamori, Y. and Spencer, B.F. (2007), "Issues in structural health monitoring employing smart sensors", *Smart Struct. Syst.*, **3**(3), 299-320.
- Ni, Y.Q., Hua, X.G., Fan, K.Q. and Ko, J.W. (2005), "Correlating modal properties with temperature using long-term monitoring data and support vector machine technique", *Eng. Struct.*, **27**, 1762-1773.
- Nguyen, K.D. and Kim, J.T. (2012), "Smart PZT-interface for wireless impedance-based prestress-loss monitoring in tendon anchorage connection", *Smart Struct. Syst.*, **9**(6), 489-504.
- Nguyen, K.D., Ho, D.D. and Kim, J.T. (2013), "Damage detection in beam-type structures via PZT's dual piezoelectric responses", *Smart Struct. Syst.*, **11**(2), 217-240.
- Park, G., Sohn, H., Farrar, C. and Inman, D. (2003), "Overview of piezoelectric impedance-based health monitoring and path forward", *Shock Vib.*, **35**(6), 451-463.
- Park, G., Cudney, H.H. and Inman, D.J. (2001), "Feasibility of using impedance-based damage assessment for pipeline structures", *Earthq. Eng. Struct. D.*, **30**(10), 1463-1474.
- Rice, J.A., Mechitov, K., Sim, S.H., Nagayama, T., Jang, S., Kim, R., Spencer, Jr, B.F., Agha, G. and Fujino, Y. (2010), "Flexible smart sensor framework for autonomous structural health monitoring", *Smart Struct. Syst.*, **6**(5-6), 423-438.
- Rice, J.A. and Spencer, B.F. (2009), *Flexible smart sensor framework for autonomous full-scale structural health monitoring*, NSEL Report Series, NSEL-018.
- Sim, S.H., Li, J., Jo, H., Park, J., Cho, S. and Spencer, B.F. (2011), "Automated cable tension monitoring using smart sensors", *Proceedings of the Advances in Structural Engineering and Mechanics*, Korea.
- Sirohi, J. and Chopra, I. (2000), "Fundamental understanding of piezoelectric strain sensors", *J. Intell. Mat. Syst. Str.*, **11**, 246-257.
- Shimada, T. (1995), *A study on the maintenance and management of the tension measurement for the cable of bridge*, PhD Dissertation, Kobe University, Japan.
- Spencer, B.F., Ruiz-Sandoval, M.E. and Kurata, N. (2004), "Smart sensing technology: opportunities and challenges", *Struct. Health Monit.*, **11**, 349-368.
- Treysede, F. (2009), "Free linear vibrations of cables under thermal stress", *J. Sound Vib.*, **327**(1-2), 1-8.
- Zui, H., Shinke, T. and Namita, Y. (1996), "Practical formulas for estimation of cable tension by vibration method", *J. Struct. Eng. - ASCE*, **122**(6), 651-656.